

1 **A novel metabarcoded DNA sequencing tool for the detection of**  
2 ***Plasmodium* species in malaria positive patients.**

3

4 Abdul Wahab<sup>a1</sup>, Ayaz Shaukat<sup>b1</sup>, Qasim Ali<sup>c1</sup>, Mubashir Hussain<sup>a</sup>, Taj Ali Khan<sup>a</sup>, M. Azmat  
5 Ullah Khan<sup>b</sup>, Imran Rashid<sup>d</sup>, Mushtaq A. Saleem<sup>b</sup>, Mike Evans<sup>e</sup>, Neil D. Sargison<sup>e\*</sup>, Umer  
6 Chaudhry<sup>f\*</sup>

7

8 <sup>a</sup> *University of Science and Technology, Kohat, Khyber Pakhtunkhwa, Pakistan*

9 <sup>b</sup> *University of Central Punjab, Lahore, Punjab, Pakistan*

10 <sup>c</sup> *Gomal University, Dera Ismail Khan, Khyber Pakhtunkhwa, Pakistan*

11 <sup>d</sup> *University of Veterinary and Animal Sciences, Lahore, Punjab, Pakistan*

12 <sup>e</sup> *Royal Dick School of Veterinary Studies, University of Edinburgh, UK*

13 <sup>f</sup> *Roslin Institute, University of Edinburgh, UK*

14

15

16 1 Contributed equally

17 \*Corresponding author:

18 Umer Chaudhry

19 Email: [uchaudhr@exseed.ed.ac.uk](mailto:uchaudhr@exseed.ed.ac.uk), Tel: 00441316519244

20 University of Edinburgh, The Roslin Institute, Easter Bush Veterinary Centre, UK, EH25  
21 9RG

22

23 Neil Sargison

24 [Neil.Sargison@ed.ac.uk](mailto:Neil.Sargison@ed.ac.uk), +44 (0)131 651 7300

25 University of Edinburgh, R(D)SVS, Easter Bush Veterinary Centre, UK, EH25 9RG

26

27

28

29

30

31

32

33

34 **Abstract**

35 Various PCR based methods have been described for the diagnosis of malaria, but most  
36 depend on the use of *Plasmodium* species-specific probes and primers; hence only the tested  
37 species are identified and there is limited available data on the true circulating species  
38 diversity. Sensitive diagnostic tools and platforms for their use are needed to detect  
39 *Plasmodium* species in both clinical cases and asymptomatic infections that contribute to  
40 disease transmission. We have been recently developed for the first time a novel high  
41 throughput ‘haemoprotozoome’ metabarcoded DNA sequencing method and applied it for the  
42 quantification of haemoprotozoan parasites (*Theileria* and *Babesia*) of livestock. Here, we  
43 describe a novel, high throughput method using an Illumina MiSeq platform to demonstrate  
44 the proportions of *Plasmodium* species in metabarcoded DNA samples derived from human  
45 malaria patients. *Plasmodium falciparum* and *Plasmodium vivax* positive control gDNA was  
46 used to prepare mock DNA pools of parasites to evaluate the detection threshold of the assay  
47 for each of the two species and to assess the accuracy of proportional quantification. We then  
48 applied the assay to malaria-positive human samples to show the species composition of  
49 *Plasmodium* communities in the Punjab province of Pakistan and in the Afghanistan-Pakistan  
50 tribal areas. The diagnostic performance of the deep amplicon sequencing method was  
51 compared to an immunochromatographic assay that is widely used in the region.  
52 Metabarcoded DNA sequencing showed better diagnostic performance, greatly increasing the  
53 estimated prevalence of *Plasmodium* infection. The next-generation sequencing method using  
54 metabarcoded DNA has potential applications in the diagnosis, surveillance, treatment, and  
55 control of *Plasmodium* infections, as well as to study the parasite biology.

56

57 **Keywords:** Malaria, *Plasmodium falciparum* and *Plasmodium vivax*, metabarcoded DNA,  
58 deep amplicon sequencing.

59

60

61

62

63

64

65

## 66 **1. Introduction**

67 Malaria is the most important vector-borne disease, causing high morbidity and mortality  
68 (Moody, 2002). More than 3.4 billion people are infected, resulting in an estimated 1.2 billion  
69 malaria cases every year (Poostchi et al., 2018). The disease is caused by intracellular  
70 protozoan parasites of the genus *Plasmodium* transmitted through *Anopheles* mosquitoes  
71 (Dash et al., 2007; Sinka et al., 2012). *Plasmodium* has an indirect life cycle including one  
72 stage in *Anopheles* mosquitoes and three different stages in humans, all with different rates of  
73 replication (Li et al., 1997). Gametogenesis occurs in human blood and fertilisation of male  
74 and female macro and microgametes occurs in the midgut of the mosquito after feeding.  
75 Asexual stages occur in the gut of the mosquito as sporogony, and after biting the humans,  
76 sporozoites undergo exoerythrocytic schizogony in the hepatic cells and then erythrocytic  
77 schizogony in the blood cells (Li et al., 1994b). Five species of *Plasmodium* parasite infect  
78 humans, namely *Plasmodium falciparum*, *Plasmodium vivax*, *Plasmodium ovale*, *Plasmodium*  
79 *malariae* and *Plasmodium knowlesi*. *P. falciparum* is the most associated with lethal disease,  
80 but in recent years, there has been an increase in disease severity attributable to *P. vivax*  
81 (Saravu et al., 2014; Scholzen et al., 2014; William et al., 2011).

82 The 18S rDNA of *Plasmodium* is unique due to its genomic arrangement dispersed among  
83 different chromosomes. The copy number is limited to 4 to 8 per genome and the sequences  
84 are not identical (Li et al., 1994b). Their expression is regulated during different development  
85 stages of the life cycle (Li et al., 2014); for example, at least three types of genotypic variants  
86 have been identified between stages of *P. falciparum* and *P. vivax* laboratory isolates (Li et  
87 al., 1994b; McCutchan et al., 1988; Qari et al., 1994; Rogers et al., 1995). However, the  
88 presence of these variants has not been reported in the field studies.

89 The 18S rDNA of *Plasmodium* forms a mosaic of conserved and variable regions;  
90 whereby the conserved regions contribute to form a secondary structure of rRNA that appears  
91 to be associated with the universal function of the ribosomes. The variable regions are  
92 scattered among the conserved regions and contribute to major differences in gene  
93 composition and size (Li et al., 1994a). The function of variable regions is not fully  
94 understood, but determination of sequence variations can discriminate between *Plasmodium*  
95 species (Agudelo et al., 2013; Haanshuus et al., 2013; Lee et al., 2015; Lefterova et al., 2015),  
96 and overcome limitations of traditional microscopic and immunochromatographic methods  
97 for the diagnosis of this group of parasites at species level.

98 Significant progress has been made in the global fight against malaria through high  
99 throughput rapid diagnosis. Sensitive diagnostic tools are needed to detect clinically and  
100 subclinically infected patients (Echeverry et al., 2016). Molecular methods including qPCR,  
101 species-specific PCR, nested PCR, and multiplex PCR have been described (Canier et al.,  
102 2013; Cunha et al., 2009; Das et al., 1995; Echeverry et al., 2016; Haanshuus et al., 2013;  
103 Steenkeste et al., 2009), but these are low throughput, hence relatively expensive (Chaudhry  
104 et al., 2019). These methods depend on the use of species-specific probes and primers,  
105 meaning that only the tested species are identified, hence are limited in their ability to  
106 describe true circulating species diversity (Moody, 2002). In contrast, high throughput  
107 metabarcoded DNA sequencing using the Illumina MiSeq platform is relatively low-cost and  
108 potentially less error-prone. We have applied this ‘haemprotobiome’ method, to the study of  
109 tick-borne haemoprotozoan parasites of ruminants (Chaudhry et al., 2019). The method has  
110 the potential to open new areas of research in the study of *Plasmodium*, to accurately provide  
111 relative quantification of co-infecting species and to evaluate drug treatment responses  
112 (Shaukat et al., 2019). The method uses primers binding to the conserved sites and analyse of  
113 up to 600 bp sequence reads. The use of adapter and barcoded primers allows a large number  
114 of samples to be pooled and sequenced in a single MiSeq flow cell, making the assay suitable  
115 for high-throughput analysis (Shaukat et al., 2019).

116 Here, we report for the first time the development of a deep sequencing method using the  
117 Illumina MiSeq platform to quantify *P. falciparum* and *P. vivax* present in malaria-positive  
118 human blood samples. The results are compared with a standard immunochromatographic  
119 assay to validate the method’s accuracy for species identification.

120

## 121 **2. Materials and methods**

122

### 123 *2.1. Parasite material*

124 Positive control samples of *P. falciparum* were kindly provided by D Jason Mooney at the  
125 Roslin Institute, University of Edinburgh, UK, previously obtained from National Institute for  
126 Biological Standards and Control (NIBSC code 04/176). *P. vivax* control samples were kindly  
127 provided by Dr Imran Rashid at the University of Veterinary and Animal Sciences, Lahore,  
128 Pakistan, previously obtained from the Biodefense and Emerging Infections Research  
129 Resources Repository (BEI code MRA-41). Four replicates each of mock pools comprising of  
130 *P. falciparum* only (Mix 1), *P. vivax* only (Mix 2), and *P. falciparum* and *P. vivax* (Mix 3)  
131 were created. These were used to test the detection threshold of the metabarcoded sequencing

132 method and to show the proportions of each of the *Plasmodium* species present. Four negative  
133 control of human blood samples were provided by Sana Amir and Saqib Shahzad, Chughtai  
134 Diagnostic Laboratory, Lahore Pakistan.

135 Malaria suspected patients referred to Basic Health Units in the tribal areas of the  
136 Afghanistan-Pakistan border and Chughtai Diagnostic Laboratory in the Punjab province of  
137 Pakistan were invited to participate in this study. Prior discussions were held with key  
138 administrative and community leaders to raise awareness of the study. Samples were taken by  
139 trained para-medical workers under the supervision of local collaborators and the Basic  
140 Health Unit or Chughtai Diagnostic Laboratory staff. The institutional review boards of the  
141 University of Central Punjab (UCP-30818), and the Kohat University of Science and  
142 Technology, Pakistan (KUST/EC/1379) approved the study. Patients of all age groups were  
143 included in this study with symptoms consistent with malaria, including vomiting, fever,  
144 headache, chills, sweats, nausea and fatigue.

145 Blood samples were collected by venipuncture during peak malaria transmission seasons  
146 between August to November 2017 and 2018. A total of 5 ml of intravenous blood was drawn  
147 into EDTA tubes and stored at -20 °C for gDNA isolation. Each sample was also routinely  
148 analysed by microscopic examination under oil immersion (x1000) of 4% Giemsa-stained  
149 blood smears for the diagnosis of malaria. The *Plasmodium* goes through different stages of  
150 their development cycle (48 hr), which gives the parasites a different visual appearance that  
151 can be observed under the microscope. These stages show the ring (Fig. 1A), trophozoite,  
152 schizont, and gametocyte appearance. Malaria case identification was based on the  
153 appearance of those stages on the microscopic examination (Fig. 1A). Overall, 365 malaria  
154 suspected positive patients were identified.

155

## 156 2.2. Immunochromatographic assay

157 The 365 malaria-positive on microscopic examination blood samples, each having an  
158 unknown level of parasitemia, were analysed using a commercial immunochromatographic  
159 rapid diagnostic test (RDT) kit. The Malaria Pf/Pv Ag Rapid Test (Healgen<sup>®</sup>; Zhejiang Orient  
160 Gene Biotech Co, Ltd) RDT kit was designed to detect *P. falciparum*-specific histidine-rich  
161 protein 2 (Pf-HRP2) and *P. vivax*-specific lactate dehydrogenase (Pv-LDH). The kit was  
162 transported and maintained at the room temperature, opened just before use to avoid humidity  
163 damage, and used in accordance with the manufacturer's recommendations. During the assay,  
164 an adequate volume of the blood sample was dispensed into the sample well 'S' of the test  
165 cassette and the lysis buffer is added to the buffer well 'B'. The buffer contains a detergent

166 that lyses the red blood cells and releases antigens, which migrate by capillary action across  
167 the strip held in the cassette. If Pf-HRP2 binds to the HRP2 gold conjugates and the  
168 immunocomplex is then captured on the membrane by the pre-coated anti-Pf-HRP2  
169 antibodies, forming a burgundy colored pf band, indicating *P. falciparum* positive test (Fig.  
170 1B). If Pv-LDH binds to the LDH gold conjugates and the immunocomplex is then captured  
171 on the membrane by the pre-coated anti-Pv-LDH antibodies, forming a burgundy colored pv  
172 band, indicating *P. vivax* positive test (Fig. 1B). The absence of any band suggests a negative  
173 result. The test also contained an internal control 'C' band, exhibiting a burgundy colored  
174 band of the immunocomplex of goat anti-mouse IgG/mouse IgG (anti-Pv-LDH and anti-Pf-  
175 HRP2) gold conjugates, regardless of the color development on 'C' band.

176

### 177 2.3. Genomic DNA isolation, primer design and adapter/barcoded PCR amplification of 178 rDNA 18S locus

179 50 µl of blood from each of the 365 samples was used as a template, to extract gDNA  
180 according to the protocols described in the TIANamp blood DNA kit (Tiangen Biotech  
181 (Beijing) Co., Ltd). Overall, 589 bp and 568 bp fragments of *P. falciparum* and *P. vivax* 18S  
182 rDNA, respectively, were amplified using newly developed adapter primer sets  
183 (Supplementary Table S1). The overall scheme of the sample preparation is described in  
184 Figure 2A. Adapters were added to these primers to allow the successive annealing of  
185 subsequent metabarcode primers and N is the number of random nucleotides included  
186 between the locus-specific primers and adapter to increase the variety of generated amplicons  
187 as previously described by Chaudhry et al. (2019). Four forward (Plasmo1\_For,  
188 Plasmo1\_For-1N, Plasmo1\_For-2N, Plasmo1\_For-3N) and four reverse (Plasmo2\_Rev,  
189 Plasmo1\_Rev-1N, Plasmo1\_Rev-2N, Plasmo1\_Rev-3N) primers were mixed in equal  
190 proportion (Supplementary Table S1) and used for first-round PCR under the following  
191 conditions: 5X KAPA buffer, 10mM dNTPs, 10 uM forward and reverse adapter primer, 0.5  
192 U KAPA Polymerase (KAPA Biosystems, USA), and 1 ul of worm lysate. The thermocycling  
193 conditions of the PCR were 95°C for 2 min, followed by 35 cycles of 98°C for 20 sec, 60°C  
194 for 15 sec, 72°C for 15 sec and a final extension 72°C for 5 min. PCR products were purified  
195 with AMPure XP Magnetic Beads (1X) (Beckman Coulter, Inc.).

196 After the purification, a second-round PCR was performed by using sixteen forward and  
197 twenty-four reverse barcoded primers. The barcoded forward (N501 to N516) and reverse  
198 (N701 to N724) primers (10 uM each) were previously described by Chaudhry et al. (2019).  
199 The primers were used in a manner that repetition of same forward and reverse sequences did

200 not occur in the different samples. The second-round PCR conditions were: 5X KAPA buffer,  
201 10 mM dNTPs 0.5 U KAPA Polymerase (KAPA Biosystems, USA), and 2 ul of first-round  
202 PCR product as DNA template. The thermocycling conditions of the second round PCR were  
203 98°C for 45 sec, followed by 7 cycles of 98°C for 20 sec, 63°C for 20 sec, and 72°C for 2  
204 minutes. PCR products were purified with AMPure XP Magnetic Beads (1X) according to the  
205 protocols described by Beckman Coulter, Inc.

206

#### 207 2.4. Sequencing of metabarcoded 18S rDNA, data handling, and bioinformatic analysis

208 The pooled library was measured with KAPA qPCR library quantification kit (KAPA  
209 Biosystems, USA). The prepared library was then run on Illumina MiSeq Sequencer using a  
210 600-cycle pair-end reagent kit (MiSeq Reagent Kits v2, MS-103-2003) at a concentration of  
211 15 nM with an addition of 25% Phix Control v3 (Illumina, FC-11-2003).

212 The overall scheme of the data handling and bioinformatics analysis is described in Figure  
213 2B. MiSeq data were handled with our own bioinformatics pipeline (Chaudhry et al., 2019).  
214 Briefly, MiSeq separates all sequence reads during post-run processing using the barcoded  
215 indices and to generate FASTQ files. The raw paired read-ends were run into the  
216 ‘make.contigs’ command to combine the two sets of reads for each sample. The command  
217 extracts sequence and quality score data from the FASTQ files, creating the complement of  
218 the reverse and forward reads, and then joining the reads into contigs. After removing the too  
219 long, or ambiguous sequence reads, the data were then aligned with the *P. falciparum* and *P.*  
220 *vivax* reference sequence library (for more details Supplementary Data S1 and Result section  
221 3.1) using the ‘align.seqs’ command to summarise the 589 bp and 568 bp fragments  
222 encompassing parts of the 18S DNA spanning the hyper-variable region of the *P. falciparum*  
223 and *P. vivax* ribosomal cistrons. At this stage, the 18S rDNA analysis was completed by  
224 classifying the sequences into either of the two species by using the ‘classify.seqs’ command  
225 and creating a taxonomy file by using the ‘summary.tax’ command. Overall, 762674 million  
226 reads of 18S rDNA were generated from the data set.

227 For the phylogenetic analysis of *P. falciparum* and *P. vivax* 18S rDNA, all the classified  
228 sequences were run on the ‘screen.seqs’ command and the count list of the consensus  
229 sequences of each sample was created using the ‘unique.seqs’ command followed by the use  
230 of the ‘pre.cluster’ command to look for sequences differences and to merge them in groups  
231 based on their abundance. Any chimeras were identified and removed by using the  
232 ‘chimera.vsearch’ command. The count list was further used to create the FASTQ files of the

233 consensus sequences of each sample using the ‘split.groups’ command (for more details  
234 Supplementary Data S2).

235

### 236 *2.5. Split and maximum-likelihood trees of P. falciparum and P. vivax 18S rDNA sequences*

237 *P. falciparum* and *P. vivax* 18S rDNA sequence reads were analysed separately in  
238 Geneious v9.0.1 software (Kearse et al., 2012) using the MUSCLE alignment tool. The  
239 aligned sequences were then imported into the FaBox 1.5 online tool to collapse those with  
240 100% base pair similarity after corrections into single genotypes. The split tree of *P.*  
241 *falciparum* and *P. vivax* 18S rDNA was created in the SplitTrees4 software by using the  
242 UPGMA method in the Jukes-Cantor model of substitution (Huson and Bryant, 2005). The  
243 maximum-likelihood tree for *P. falciparum* and *P. vivax* 18S rDNA was constructed by the  
244 HKY model of substitution in the MEGA 7 software and to select the appropriate model of  
245 nucleotide substitutions (Tamura et al., 2013).

246

### 247 *2.6. Statistical analysis*

248 The data were analysed using CompareTests: Correct for Verification Bias in Diagnostic  
249 Accuracy and Agreement Statistics software (R package version 1.2.). The frequency of *P.*  
250 *falciparum* and *P. vivax* in the samples was calculated by dividing the number of sequence  
251 reads for each sample by the total number of reads. The effect of the mock pools of *P.*  
252 *falciparum* and *P. vivax* positive controls were analysed by running a Kruskal-Wallis rank-  
253 sum test for each admixture. The performance of the immunochromatographic assay was  
254 compared against metabarcoded sequencing, using a Fisher’s Exact test to calculate the  
255 predictive value and Category-Specific Classification Probability (CSCP) with 95%  
256 confidence interval. Kappa (k) values were calculated to express the agreement beyond  
257 chance; where values greater than 0.80 were considered to represent perfect agreement;  
258 values of 0.61 - 0.80 to represent good agreement; and values of 0.21 - 0.60 to represent  
259 moderate agreement.

260

## 261 **3. Results**

262

### 263 *3.1. P. falciparum and P. vivax 18S rDNA reference sequence libraries*

264 The sequence reads generated by metabarcoded 18S rDNA sequencing of the *P.*  
265 *falciparum* and *P. vivax* positive controls were compared to the malaria-positive samples and  
266 to the published NCBI GenBank 18S rDNA sequences to account for any genetic diversity. A



267 total of 34 *P. falciparum* and 74 *P. vivax* reference sequences were identified (Fig. 3,  
268 Supplementary Data S1). The maximum-likelihood tree shows distinct clustering of the *P.*  
269 *falciparum* and *P. vivax* 18S rDNA regions (Fig. 3), hence these closely related *Plasmodium*  
270 species can be reliably differentiated by virtue of 18S rDNA sequence variations.

271

### 272 3.2. Validation of the metabarcoded sequencing assay using mock pools of *P. falciparum* and 273 *P. vivax*

274 Four replicates each of *P. falciparum* only (Mix 1), *P. vivax* only (Mix 2), and *P.*  
275 *falciparum* and *P. vivax* (Mix 3) were created from gDNA to demonstrate the detection  
276 accuracy of the metabarcoded DNA sequencing method and to show the proportions of each  
277 of the species being present (Fig. 4; Supplementary Table S2). The mixing of different mock  
278 pools demonstrates the accurate detection ability of the metabarcoded sequencing method and  
279 to show the proportions of each of the species being present. The Mix 1 pool yielded only *P.*  
280 *falciparum* sequence reads and the Mix 2 pool yielded only *P. vivax* sequence reads (Fig. 4).  
281 The Mix 3 pool yielded both *P. falciparum* and *P. vivax* sequence reads, with no statistically  
282 significant variations between replicates (Kruskal-Wallis rank-sum test; Mix1:  $\chi^2(1) 0$ ,  $p=1$ ;  
283 Mix2:  $\chi^2(1) 0$ ,  $p=1$ ; Mix3:  $\chi^2(3) 0.02153$ ,  $p=0.5231$ ).

284

### 285 3.3. Assessment of the immunochromatographic assay and metabarcoded sequencing for the 286 identification of *P. falciparum* and *P. vivax*

287 The immunochromatographic assay and metabarcoded DNA sequencing methods were  
288 applied to malaria-positive blood samples to detect *P. falciparum* and *P. vivax* in the field  
289 (Fig. 5, Supplementary Table S3). The results of both assays demonstrate that the prevalence  
290 of *P. vivax* infection was higher than that of *P. falciparum* infection. In the case of the  
291 metabarcoded DNA sequencing assay, those samples yielding more than 1000 reads  
292 (implying sufficient gDNA for accurate amplification) were included in the analysis  
293 (Supplementary Table S3). *Plasmodium vivax* was present in 199 (69.8%) patients, *P.*  
294 *falciparum* in 84 (29.5%) and mixed infection in 2 (0.7%) patients (Fig. 5). The  
295 immunochromatographic assay showed that *Plasmodium vivax* was present in 187 (65.6%)  
296 patients, *P. falciparum* in 78 (27.4%), mixed infection in 2 (0.7%) patients (Fig. 5) and 18  
297 (6.32%) malaria-positive cases were negative in RDT, but positive in the metabarcoded DNA  
298 sequencing assay (Fig. 5).

299 The degree of agreement between the immunochromatographic and metabarcoded DNA  
300 sequencing assays was high with  $\kappa = 0.893$  (95% CI: 0.839-0.930). The Category-Specific

301 Classification Probability (CSCP) was also high in all four categories, ranging from 0.892  
302 (95% CI: 0.807 - 0.943) to 1. The Predictive Values (PV) for ‘positive RDT’ results were also  
303 very high, ranging from 0.962 (0.860 - 0.990) to 1. However, the PVs for ‘negative RDT’  
304 results were 0.816 (0.724 - 0.883); being significantly lower than the Predictive Value for  
305 both ‘RDT *P. falciparum*’ (p=0.004) and ‘RDT *P. vivax*’ (p<0.001) results. In samples with  
306 similar disease prevalence, there is, therefore, an increased likelihood that a negative RDT  
307 result may be incorrect.

308

### 309 3.4. Phylogenetic analysis of the *P. falciparum* and *P. vivax* rDNA 18S sequences

310 Overall, 112 different genotypes of the *P. falciparum* 18S rDNA locus were identified  
311 among 84 field samples and 12 from the NCBI GenBank sequences (Supplementary Data S2  
312 and section 3.1. and 3.3). The split tree shows at least two distinct clades (Fig. 6A), and it sets  
313 apart that 9 genotypes in the Clade I, belongs to a ‘type S’ 18S rDNA region (McCutchan et  
314 al., 1988). The remaining 115 genotypes were in clade II, belonging to a ‘type A’ 18S rDNA  
315 region (McCutchan et al., 1988). 80 genotypes predominated in group 1 and 35 genotypes in  
316 group 2 (Fig. 6A). In contrast, 30 different genotypes of the *P. vivax* 18S rDNA locus was  
317 identified among 199 field samples and 18 from the NCBI GenBank sequences  
318 (Supplementary Data S2 and section 3.1. and 3.3). The split tree shows at least two distinct  
319 clades (Fig. 6B), and it sets apart that 3 genotypes in the Clade I, belong to the ‘type S’ 18S  
320 rDNA as described by Li et al. (1994). The remaining 45 genotypes were in clade II,  
321 belonging to ‘type A’ 18S rDNA (Li et al., 1994b). 7 genotypes predominated in groups 1  
322 and 2, and 31 genotypes in group 3 (Fig. 6B).

323

## 324 4. Discussion

325 Microscopic examination of blood smears remains the mainstay for the diagnosis of  
326 *Plasmodium* in the field. The procedure allows the detection of levels of at least 200  
327 parasites/ul, which is sufficient for the diagnosis of most symptomatic cases, but can result in  
328 misdiagnoses at low levels of parasitemia (Rakotonirina et al., 2008; Wongsrichanalai et al.,  
329 2007). The method is labor-intensive, time-consuming, and interpretation of results requires  
330 highly skilled microscopists (Canier et al., 2013; Echeverry et al., 2016).

331 The immunochromatographic assay is also utilised in case investigation and malaria  
332 surveillance programs in the field. The method depends on the incorporation of conjugated  
333 monoclonal antibodies providing the indicator of infection (Moody, 2002; Wongsrichanalai et  
334 al., 2007). The targeted antigens are abundant in the sexual and asexual stages of the parasites,

335 while histidine-rich protein 2 (Pf-HRP2) based RDT is specific for *P. falciparum* and lactate  
336 dehydrogenase (Pf-LDH & Pv-LDH) specific for detecting both *P. falciparum* and *P. vivax*.  
337 Pan based RDT targets specific antigens including lactate dehydrogenase (P-LDH) and  
338 aldolase proteins found in all *Plasmodium* species (Akinyi Okoth et al., 2015; Murillo Solano  
339 et al., 2015). Several factors potentially affect the accuracy and false-negative results of RDT  
340 including the interpretation of the test strip colour change, the density of malaria infection in  
341 the host, improper storage/handling of the kit and poor test performance (Echeverry et al.,  
342 2016). Besides this, other major factors such cross-reactivity of HRP2 with histidine-rich  
343 protein 3 (a structural homolog with significant sequence similarity) and deletions in the  
344 HRP2 locus in *P. falciparum* isolates may account for false-negative results (Akinyi Okoth et  
345 al., 2015; Rachid Viana et al., 2017).

346 Conventional PCR based molecular methods are useful in the detection of *Plasmodium*  
347 species for which the reagents and conditions have been developed, but have limitations in  
348 terms of lacking scalability (Canier et al., 2013; Cunha et al., 2009; Das et al., 1995;  
349 Echeverry et al., 2016; Haanshuus et al., 2013; Steenkeste et al., 2009). The diagnostic  
350 challenges of the disease identification have not been resolved yet (Wongsrichanalai et al.,  
351 2007), therefore the metabarcod DNA sequencing potentially provides a more accurate and  
352 reliable automated high-throughput method to detect *Plasmodium* species in blood samples.  
353 The use of a single PCR utilising primers conserved between *Plasmodium* species provides a  
354 powerful tool to measure the relative sequence representation of each species in the blood  
355 samples. In the present study, we have evaluated a metabarcoded DNA sequencing method to  
356 identify the presence of *P. falciparum* and *P. vivax* using mock parasite pools, applying the  
357 method to malaria-positive blood samples, and the detection *P. falciparum* and *P. vivax*  
358 rDNA18S genotypic variants in the field samples.

359 We tested the ability of the metabarcoded DNA sequencing assay to accurately determine  
360 the relative species proportions in combinations of *P. falciparum* and *P. vivax*. To do this, we  
361 generated mock pools containing different estimated proportions of both species and  
362 demonstrated no significant variations between replicates. A previous study using pools of  
363 laboratory-maintained *Theileria* and *Babesia* haemoprotozoan parasites showed that the  
364 relative sequence representation was unaffected by either the number of PCR cycles  
365 employed or the parasite species composition of the sample. This study also found no  
366 sequence representation bias in PCR products used for sequencing, arising from the number  
367 of first-round PCR cycles (Chaudhry et al., 2019).

368 After validating the metabarcoded DNA sequencing assay using mock pools of  
369 *Plasmodium* positive DNA, we applied the method to field samples collected from suspected  
370 malaria-positive patients in the tribal area of the Afghanistan-Pakistan border and in the  
371 Punjab province of Pakistan, where malaria caused by *P. falciparum* and *P. vivax* has been  
372 reported (Kakar et al., 2010; Khattak et al., 2013). Our findings support previous reports of  
373 the high prevalence of malaria in the tribal areas of the Afghanistan-Pakistan border, and  
374 increasing prevalence over the last few decades in the Punjab province (Kakar et al., 2010;  
375 Khattak et al., 2013). Our results support the reports suggesting that while the majority of the  
376 cases of malaria are caused by *P. vivax*, the prevalence of *P. falciparum* has increased during  
377 recent years (Khattak et al., 2013). The increased prevalence of *P. falciparum* may be an  
378 attribute to antimicrobial resistance; previous studies have shown that the pyrimethamine and  
379 chloroquine resistance mutations in *P. falciparum* are present in different cities of Pakistan  
380 (Ghanchi et al., 2011). Another explanation for the increased prevalence of *P. falciparum* may  
381 be provided by the influx of people and the movement of refugees from areas of Afghanistan  
382 where the parasite species is common (Howard et al., 2011).

383 Three structurally distinct types of rDNA 18S genotypic variants have been reported in *P.*  
384 *falciparum* and *P. vivax* laboratory isolates (Li et al., 1994b; McCutchan et al., 1988; Qari et  
385 al., 1994; Rogers et al., 1995). The existence of genotypic variants in the field studies has not  
386 been described. In the present study, we have identified the two independent gene duplication  
387 events that occurred in *P. falciparum*, leading to the A and S type rDNA18S lineages; the type  
388 A lineage being the ancestor of at least two groups (Fig. 6A). In *P. vivax*, we identified two  
389 independent gene duplication events, also leading to the A and S type rDNA18S lineages; the  
390 type A lineage being the ancestor of at least three groups (Fig. 6B). In the previous reports,  
391 type A was transcribed in erythrocytic schizogony and gametocyte stages consistent with  
392 those stages that could have been represented in the present study. In these reports, type S was  
393 transcribed in the exoerythrocytic schizogony stage, while type O was associated with oocyst  
394 development only in infected mosquitoes (Li et al., 1997). These observed differences in the  
395 18S loci of *P. falciparum* and *P. vivax* field samples confirm the presence of genotypic  
396 variants. Better understanding is needed of the function of these structurally distinct  
397 ribosomes that are active with enhanced transcription during different stages of parasitic  
398 development in *Plasmodium*, with reference to the development of disease control strategies.

399 In conclusion, we describe for the first time the use of metabarcoded DNA sequencing  
400 using an Illumina MiSeq platform to quantify *P. falciparum* and *P. vivax*, and demonstrate its  
401 accuracy on malaria-positive samples. Our results provide a proof of concept for the use of

402 the method in disease surveillance, similar to its application in the study of haemoprotozoan  
403 parasites of livestock (Chaudhry et al., 2019) and dogs (Huggins et al., 2019). This work was  
404 undertaken to explore the possibilities for the application of this high throughput method to  
405 determine the dynamics of co-infections, disease biology and epidemiology in *Plasmodium*  
406 parasites, and has applications in monitoring the changes in parasite populations after the  
407 emergence and spread of antimicrobial drug resistance (Shaukat et al., 2019).

#### 408 **Acknowledgment**

409 The study was financially supported by the Roslin Institute uses facilities funded by the  
410 Biotechnology and Biological Sciences Research Council (BBSRC). Work at the University  
411 of Veterinary and Animal Science Pakistan and Kohat University of Science and Technology  
412 Pakistan uses facilities funded by the Higher Education Commission of Pakistan.

413

#### 414 **Conflict of interest**

415 None

416

#### 417 **References**

- 418 Agudelo, O., Arango, E., Maestre, A., Carmona-Fonseca, J., 2013. Prevalence of gestational, placental  
419 and congenital malaria in north-west Colombia. *Malar. J.* 12, 1475-2875.
- 420 Akinyi Okoth, S., Abdallah, J.F., Ceron, N., Adhin, M.R., Chandrabose, J., Krishnalall, K., Huber,  
421 C.S., Goldman, I.F., Macedo de Oliveira, A., Barnwell, J.W., Udhayakumar, V., 2015.  
422 Variation in *Plasmodium falciparum* histidine-rich protein 2 (Pfhrp2) and *Plasmodium*  
423 *falciparum* histidine-rich protein 3 (Pfhrp3) gene deletions in Guyana and Suriname. *PLoS*  
424 *One.* 10, e0126805.
- 425 Canier, L., Khim, N., Kim, S., Sluydts, V., Heng, S., Dourng, D., Eam, R., Chy, S., Khean, C., Loch,  
426 K., Ken, M., Lim, H., Siv, S., Tho, S., Masse-Navette, P., Gryseels, C., Uk, S., Van Roey, K.,  
427 Grietens, K.P., Sokny, M., Thavrin, B., Chuor, C.M., Deubel, V., Durnez, L., Coosemans, M.,  
428 Menard, D., 2013. An innovative tool for moving malaria PCR detection of parasite reservoir  
429 into the field. *Malar. J.* 12, 405.
- 430 Chaudhry, U., Ali, Q., Rashid, I., Shabbir, M.Z., Ijaz, M., Abbas, M., Evans, M., Ashraf, K., Morrison,  
431 I., Morrison, L., Sargison, N.D., 2019. Development of a deep amplicon sequencing method to  
432 determine the species composition of piroplasm haemoprotozoa. *Ticks Tick Borne Dis.* 10,  
433 101276.
- 434 Cunha, M.G., Medina, T.S., Oliveira, S.G., Marinho, A.N., Povoia, M.M., Ribeiro-dos-Santos, A.K.,  
435 2009. Development of a Polymerase Chain Reaction (PCR) method based on amplification of  
436 mitochondrial DNA to detect *Plasmodium falciparum* and *Plasmodium vivax*. *Acta Trop.* 111,  
437 35-38.
- 438 Das, A., Holloway, B., Collins, W.E., Shama, V.P., Ghosh, S.K., Sinha, S., Hasnain, S.E., Talwar,  
439 G.P., Lal, A.A., 1995. Species-specific 18S rRNA gene amplification for the detection of *P.*  
440 *falciparum* and *P. vivax* malaria parasites. *Mol. Cell. Probes.* 9, 161-165.
- 441 Dash, A., Adak, T., Raghavendra, K., Singh, O., 2007. The biology and control of malaria vectors.  
442 *Curr Sci* 92, 1571-1578.
- 443 Echeverry, D.F., Deason, N.A., Davidson, J., Makuru, V., Xiao, H., Niedbalski, J., Kern, M., Russell,  
444 T.L., Burkot, T.R., Collins, F.H., Lobo, N.F., 2016. Human malaria diagnosis using a single-

- 445 step direct-PCR based on the *Plasmodium* cytochrome oxidase III gene. *Malar. J.* 15, 016-  
446 1185.
- 447 Ghanchi, N.K., Ursing, J., Beg, M.A., Veiga, M.I., Jafri, S., Martensson, A., 2011. Prevalence of  
448 resistance associated polymorphisms in *Plasmodium falciparum* field isolates from southern  
449 Pakistan. *Malar. J.* 10, 18.
- 450 Haanshuus, C.G., Mohn, S.C., Morch, K., Langeland, N., Blomberg, B., Hanevik, K., 2013. A novel,  
451 single-amplification PCR targeting mitochondrial genome highly sensitive and specific in  
452 diagnosing malaria among returned travellers in Bergen, Norway. *Malar. J.* 12, 1475-2875.
- 453 Howard, N., Durrani, N., Sanda, S., Beshir, K., Hallett, R., Rowland, M., 2011. Clinical trial of  
454 extended-dose chloroquine for treatment of resistant falciparum malaria among Afghan  
455 refugees in Pakistan. *Malar. J.* 10, 171.
- 456 Huggins, L.G., Koehler, A.V., Ng-Nguyen, D., Wilcox, S., Schunack, B., Inpankaew, T., Traub, R.J.,  
457 2019. A novel metabarcoding diagnostic tool to explore protozoan haemoparasite diversity in  
458 mammals: a proof-of-concept study using canines from the tropics. *Scientific Reports* 9,  
459 12644.
- 460 Huson, D.H., Bryant, D., 2005. Application of phylogenetic networks in evolutionary studies. *Mol.*  
461 *Biol. Evol.* 23, 254-267.
- 462 Kakar, Q., Khan, M.A., Bile, K.M., 2010. Malaria control in Pakistan: new tools at hand but  
463 challenging epidemiological realities. *East Mediterr Health J.* 16, S54-60.
- 464 Kearse, M., Moir, R., Wilson, A., Stones-Havas, S., Cheung, M., Sturrock, S., Buxton, S., Cooper, A.,  
465 Markowitz, S., Duran, C., 2012. Geneious Basic: an integrated and extendable desktop  
466 software platform for the organization and analysis of sequence data. *Bioinformatics.* 28,  
467 1647-1649.
- 468 Khattak, A.A., Venkatesan, M., Nadeem, M.F., Satti, H.S., Yaqoob, A., Strauss, K., Khatoon, L.,  
469 Malik, S.A., Plowe, C.V., 2013. Prevalence and distribution of human *Plasmodium* infection  
470 in Pakistan. *Malar. J.* 12, 1475-2875.
- 471 Kozich, J.J., Westcott, S.L., Baxter, N.T., Highlander, S.K., Schloss, P.D., 2013. Development of a  
472 dual-index sequencing strategy and curation pipeline for analyzing amplicon sequence data on  
473 the miseq illumina sequencing platform. *Appl. Environ. Microbiol.* 79, 5112-20.
- 474 Lee, P.C., Chong, E.T., Anderios, F., Al Lim, Y., Chew, C.H., Chua, K.H., 2015. Molecular detection  
475 of human *Plasmodium* species in Sabah using PlasmoNex multiplex PCR and hydrolysis  
476 probes real-time PCR. *Malar. J.* 14, 015-0542.
- 477 Lefterova, M.I., Budvytiene, I., Sandlund, J., Farnert, A., Banaei, N., 2015. Simple Real-Time PCR  
478 and Amplicon Sequencing Method for Identification of *Plasmodium* Species in Human Whole  
479 Blood. *J. Clin. Microbiol.* 53, 2251-2257.
- 480 Li, J., Gutell, R.R., Damberger, S.H., Wirtz, R.A., Kissinger, J.C., Rogers, M.J., Sattabongkot, J.,  
481 McCutchan, T.F., 1997. Regulation and trafficking of three distinct 18 S ribosomal RNAs  
482 during development of the malaria parasite. *J. Mol. Biol.* 269, 203-213.
- 483 Li, J., McConkey, G.A., Rogers, M.J., Waters, A.P., McCutchan, T.R., 1994a. *Plasmodium*: the  
484 developmentally regulated ribosome. *Exp. Parasitol.* 78, 437-441.
- 485 Li, J., Wirtz, R.A., McConkey, G.A., Sattabongkot, J., McCutchan, T.F., 1994. Transition of  
486 *Plasmodium vivax* ribosome types corresponds to sporozoite differentiation in the mosquito.  
487 *Mol. Biochem. Parasitol.* 65, 283-289.
- 488 Li, M., Xia, Z., Yan, H., 2014. New type of SSUrDNA sequence was detected from both *Plasmodium*  
489 *ovale curtisi* and *Plasmodium ovale wallikeri* samples. *Malar. J.* 13, 216.
- 490 McCutchan, T.F., de la Cruz, V.F., Lal, A.A., Gunderson, J.H., Elwood, H.J., Sogin, M.L., 1988.  
491 Primary sequences of two small subunit ribosomal RNA genes from *Plasmodium falciparum*.  
492 *Mol. Biochem. Parasitol.* 28, 63-68.
- 493 Moody, A., 2002. Rapid diagnostic tests for malaria parasites. *Clin. Microbiol. Rev.* 15, 66-78.
- 494 Murillo Solano, C., Akinyi Okoth, S., Abdallah, J.F., Pava, Z., Dorado, E., Incardona, S., Huber, C.S.,  
495 Macedo de Oliveira, A., Bell, D., Udhayakumar, V., Barnwell, J.W., 2015. Deletion of  
496 *Plasmodium falciparum* histidine-rich protein 2 (pfrp2) and histidine-rich protein 3 (pfrp3)  
497 genes in Colombian Parasites. *PLoS One.* 10, e0131576.
- 498 Poostchi, M., Silamut, K., Maude, R.J., Jaeger, S., Thoma, G., 2018. Image analysis and machine  
499 learning for detecting malaria. *Transl Res.* 194, 36-55.

- 500 Qari, S.H., Goldman, I.F., Pieniazek, N.J., Collins, W.E., Lal, A.A., 1994. Blood and sporozoite stage-  
501 specific small subunit ribosomal RNA-encoding genes of the human malaria parasite  
502 *Plasmodium vivax*. *Gene*. 150, 43-49.
- 503 Rachid Viana, G.M., Akinyi Okoth, S., Silva-Flannery, L., Lima Barbosa, D.R., Macedo de Oliveira,  
504 A., Goldman, I.F., Morton, L.C., Huber, C., Anez, A., Dantas Machado, R.L., Aranha  
505 Camargo, L.M., Costa Negreiros do Valle, S., Marins Povoas, M., Udhayakumar, V., Barnwell,  
506 J.W., 2017. Histidine-rich protein 2 (pfrhp2) and pfrhp3 gene deletions in *Plasmodium*  
507 *falciparum* isolates from select sites in Brazil and Bolivia. *PLoS One*. 12, e01711150.
- 508 Rakotonirina, H., Barnadas, C., Raheerijafy, R., Andrianantenaina, H., Ratsimbaoa, A., Randrianasolo,  
509 L., Jahevitra, M., Andriantsoanirina, V., Menard, D., 2008. Accuracy and reliability of malaria  
510 diagnostic techniques for guiding febrile outpatient treatment in malaria-endemic countries.  
511 *Am. J. Trop. Med. Hyg.* 78, 217-221.
- 512 Rogers, M.J., McConkey, G.A., Li, J., McCutchan, T.F., 1995. The ribosomal DNA loci in  
513 *Plasmodium falciparum* accumulate mutations independently. *J. Mol. Biol.* 254, 881-891.
- 514 Saravu, K., Rishikesh, K., Kamath, A., Shastry, A.B., 2014. Severity in *Plasmodium vivax* malaria  
515 claiming global vigilance and exploration-a tertiary care centre-based cohort study. *Malar. J.*  
516 13, 10.1186.
- 517 Schloss, P.D., Westcott, S.L., Ryabin, T., Hall, J.R., Hartmann, M., Hollister, E.B., Lesniewski, R.A.,  
518 Oakley, B.B., Parks, D.H., Robinson, C.J., Sahl, J.W., Stres, B., Thallinger, G.G., Van Horn,  
519 D.J., Weber, C.F., 2009. Introducing mothur: open-source, platform-independent, community-  
520 supported software for describing and comparing microbial communities. *Appl. Environ.*  
521 *Microbiol.* 75, 7537-7541.
- 522 Scholzen, A., Cooke, B.M., Plebanski, M., 2014. *Plasmodium falciparum* induces Foxp3hi CD4 T  
523 cells independent of surface PfEMP1 expression via small soluble parasite components. *Front.*  
524 *Microbiol.* 5, 200.
- 525 Shaukat, A., Ali, Q., Connelley, T., Khan, M.A.U., Saleem, M.A., Evans, M., Rashid, I., Sargison,  
526 N.D., Chaudhry, U., 2019. Selective sweep and phylogenetic models for the emergence and  
527 spread of pyrimethamine resistance mutations in *Plasmodium vivax*. *Infect. Genet. Evol.* 68,  
528 221-230.
- 529 Sinka, M.E., Bangs, M.J., Manguin, S., Rubio-Palis, Y., Chareonviriyaphap, T., Coetzee, M., Mbogo,  
530 C.M., Hemingway, J., Patil, A.P., Temperley, W.H., 2012. A global map of dominant malaria  
531 vectors. *Parasit. Vectors*. 5, 69.
- 532 Steenkeste, N., Incardona, S., Chy, S., Duval, L., Ekala, M.T., Lim, P., Hewitt, S., Sochantha, T.,  
533 Socheat, D., Rogier, C., Mercereau-Puijalon, O., Fandeur, T., Ariey, F., 2009. Towards high-  
534 throughput molecular detection of *Plasmodium*: new approaches and molecular markers.  
535 *Malar. J.* 8, 1475-2875.
- 536 Tamura, K., Stecher, G., Peterson, D., Filipowski, A., Kumar, S., 2013. MEGA6: molecular evolutionary  
537 genetics analysis version 6.0. *Mol. Biol. Evol.* 30, 2725-2729.
- 538 William, T., Menon, J., Rajahram, G., Chan, L., Ma, G., Donaldson, S., Khoo, S., Frederick, C., Jelip,  
539 J., Anstey, N.M., 2011. Severe *Plasmodium knowlesi* malaria in a tertiary care hospital, Sabah,  
540 Malaysia. *Emerg. Infect. Dis.* 17, 1248-1255.
- 541 Wongsrichanalai, C., Barcus, M.J., Muth, S., Sutamihardja, A., Wernsdorfer, W.H., 2007. A review of  
542 malaria diagnostic tools: microscopy and rapid diagnostic test (RDT). *Am. J. Trop. Med. Hyg.*  
543 77, 119-127.

544

## 545 **Figure Legends**

546 **Fig.1.** (A) Giemsa-stained blood smears were examined by 1000 x microscopy, showing rings  
547 in the *Plasmodium* positive samples. (B) Immunochromatographic assay for the detection of  
548 *P. falciparum* specific histidine-rich protein 2 (Pf-HRP2) and *P. vivax* specific lactate  
549 dehydrogenase (Pv-LDH). Adequate volumes of the blood samples were dispensed into the  
550 sample well 'S' of the test cassette. If Pf-HRP2 was bind to the HRP2 gold conjugates

551 forming a burgundy colored pf band, indicating *P. falciparum* positive test. If Pv-LDH was  
552 bind to the LDH gold conjugates forming a burgundy colored pv band, indicating *P. vivax*  
553 positive test. The absence of any band suggests a negative result and C is positive control.

554

555 **Fig. 2.** Schematic representation of the sample preparation (A) and the bioinformatics data  
556 handling (B) of the metabarcoded sequencing library. (A) In the first-round PCR  
557 amplification, overhanging forward and reverse primers were used to amplify the rDNA 18S.  
558 The adapter base pairs provide the target sites for the primers used for sequencing and the  
559 random nucleotides (0-3Ns) were inserted between the primers and the adapter to offset the  
560 reading frame, therefore amplicons prevent the oversaturation of the MiSeq sequencing  
561 channels. The second-round PCR amplification was then performed using overhanging  
562 barcoded primers bound to the adapter tags to add indices, as well as the P7 and P5 regions  
563 required to bind to the MiSeq flow cell. (B) Text files containing rDNA 18S sequence data  
564 (FASTQ files) were generated from the Illumina MiSeq binary raw data outputs, and data  
565 analyses were performed using a bespoke modified pipeline in Mothur v1.39.5 software  
566 (Schloss et al., 2009) and Illumina MiSeq standard procedures (Kozich et al., 2013) as  
567 described in materials and methods section 2.4.

568

569 **Fig. 3.** The maximum-likelihood tree was obtained from the *P. falciparum* and *P. vivax* rDNA  
570 18S region. The sequences were first calculated the number of reference sequences generated  
571 from both species (Supplementary Data S1). A total of 34 reference sequences of the rDNA  
572 18S locus were identified in *P. falciparum* and 74 reference sequences were identified in *P.*  
573 *vivax*. The reference sequences were aligned on the MUSCLE tool of the Geneious v9.0.1  
574 software. The neighbor-joining algorithm (HKY parameter model) was computed with 1000  
575 bootstrap replicates using MEGA 7 software. Both species were identified with different color  
576 shades (*P. falciparum* in blue and *P. vivax* in brown).

577

578 **Fig. 4.** Validation of the metabarcoding sequencing using three separate mock pools [Mix 1  
579 (*P. falciparum*), Mix 2 (*P. vivax*), Mix 3 (*P. falciparum* and *P. vivax*)] of unknown numbers  
580 of parasites from each species. Panel 2A shows that metabarcoded sequencing was used on  
581 four replicates of each mock pool to amplify both species as denoted on the X-axis. The Y-  
582 axis shows the percentage proportions of each species. Panel 2B shows how the replicates  
583 were grouped and averaged based on the amplification. The species are identified with  
584 different colours (*P. falciparum* in blue and *P. vivax* in brown).

585

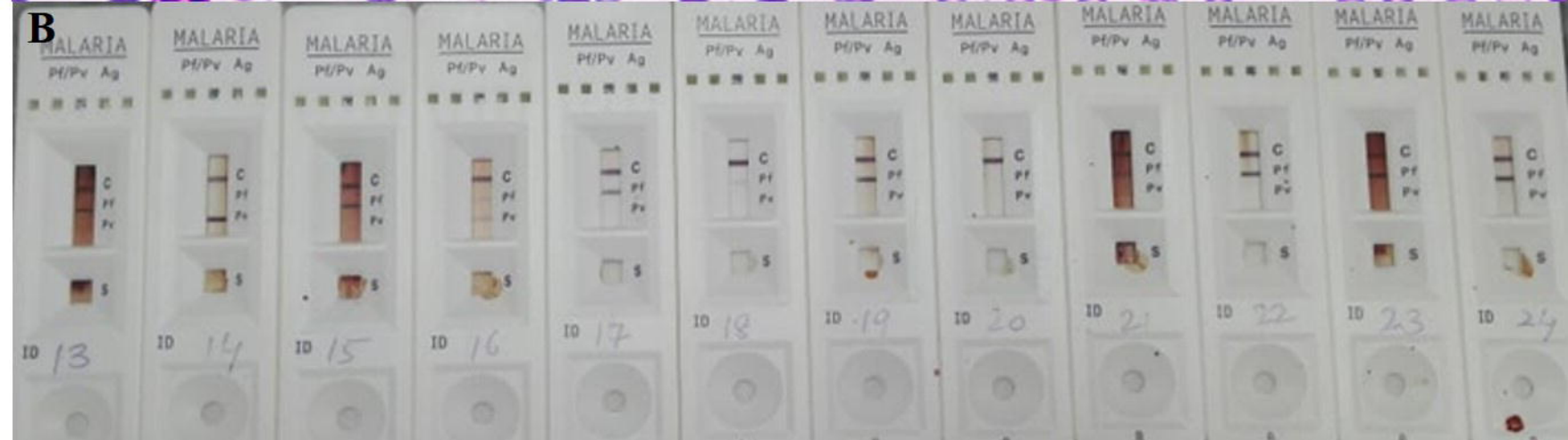
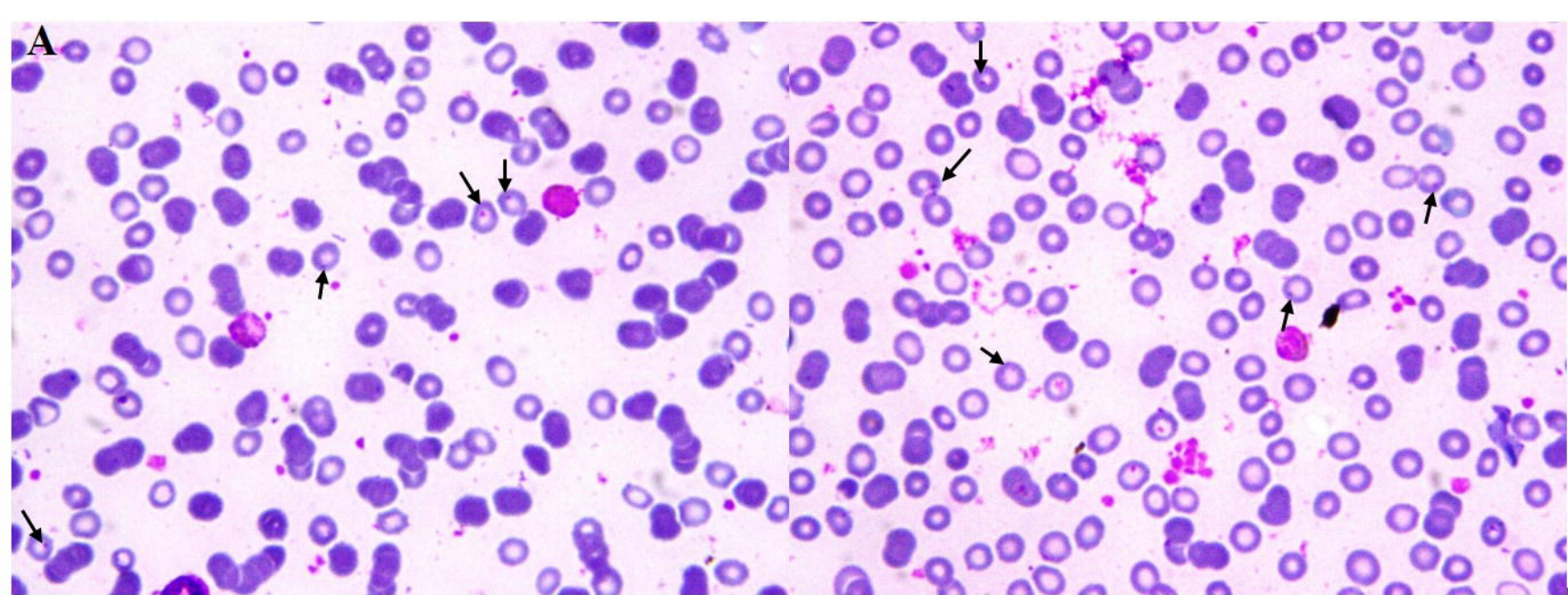
586 **Fig. 5.** Immunochromatographic assay (RDT) and the metabarcoding sequencing (Illumina  
587 MiSeq) was performed for the detection of *P. falciparum* and *P. vivax*. A total of 365 malaria-  
588 positive samples were collected in EDTA tube from basic health units in the tribal area of the  
589 Pakistan-Afghanistan border and Chughtai Diagnostic Laboratory in the Punjab province of  
590 Pakistan. The immunochromatographic assay and the metabarcoded 18S rDNA sequencing  
591 methods were applied to each sample; the X-axis shows the proportion of each species being  
592 estimated and the Y-axis shows the percentage proportions of each species. The species are  
593 identified with different colours (*P. falciparum* in pink and *P. vivax* in light blue).

594

595 **Fig. 6.** Split tree was made for the *P. falciparum* and *P. vivax* 18S rDNA sequence data. 134  
596 genotypes were identified in *P. falciparum* and 48 genotypes were identified in *P. vivax*  
597 (Supplementary Data S2). The genotypes were aligned on the MUSCLE tool of the Geneious  
598 v9.0.1 and the tree was constructed with the UPGMA method in the Jukes-Cantor model of  
599 substitution in the SplitsTrees4 software. The appropriate model of nucleotide substitutions  
600 was selected by using the jModeltest 13.1.0 program. The pie chart circles in the tree

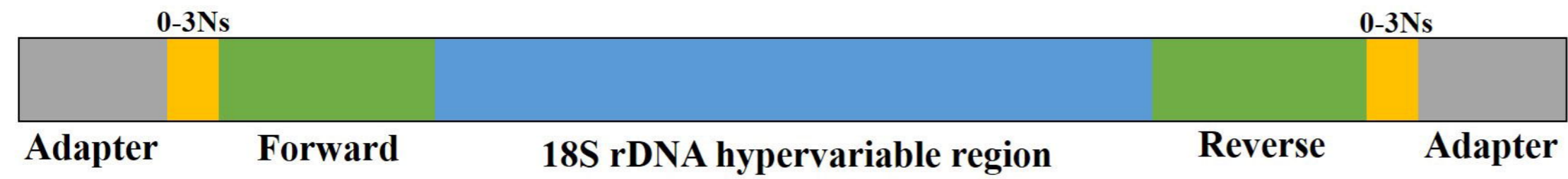


601 represent the different 18S genotypes containing different colours as follows: (A) *P.*  
602 *falciparum* from the field samples are coloured pink (type A group 1 and 2) and NCBI  
603 database sequences are coloured blue (type A group 1 and type S). (B) *P. vivax* from the field  
604 samples are coloured light blue (type A group 1, 2 and 3) and NCBI database sequences are  
605 coloured brown (type A group 3 and type S).



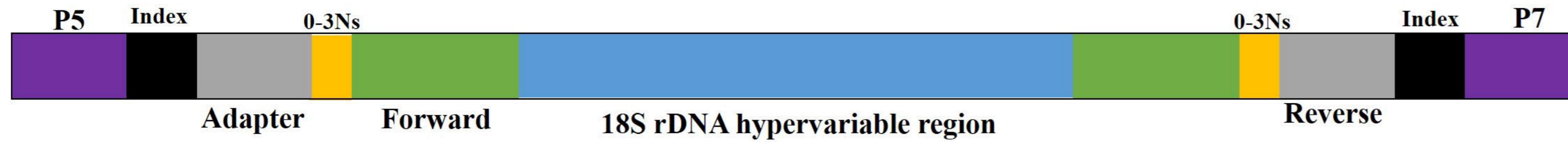
## (A) Sample preparation

### 1. Adapter PCR

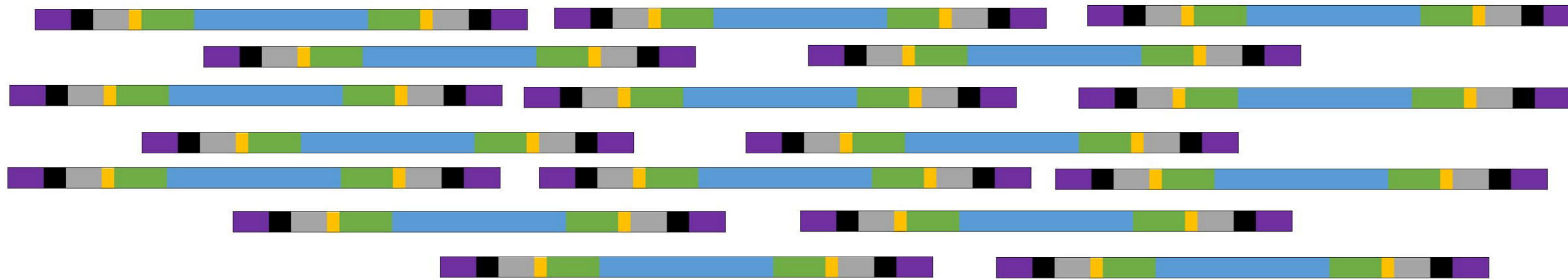


bioRxiv preprint doi: <https://doi.org/10.1101/801175>; this version posted November 15, 2019. The copyright holder for this preprint (which was not certified by peer review) is the author/funder. All rights reserved. No reuse allowed without permission.

### 2. Barcoded PCR



### 3. Pooling of all samples



### 4. Sequencing each sample on Illumina MiSeq platform



## (B) Bioinformatics data handling

### Step 1

Raw paired-ends reads were analysed  
(make.contigs' command)

Remove any ambiguous bases  
(screen.seqs command)

Align dataset with a rDNA 18S reference  
sequence library  
(align.seqs command)

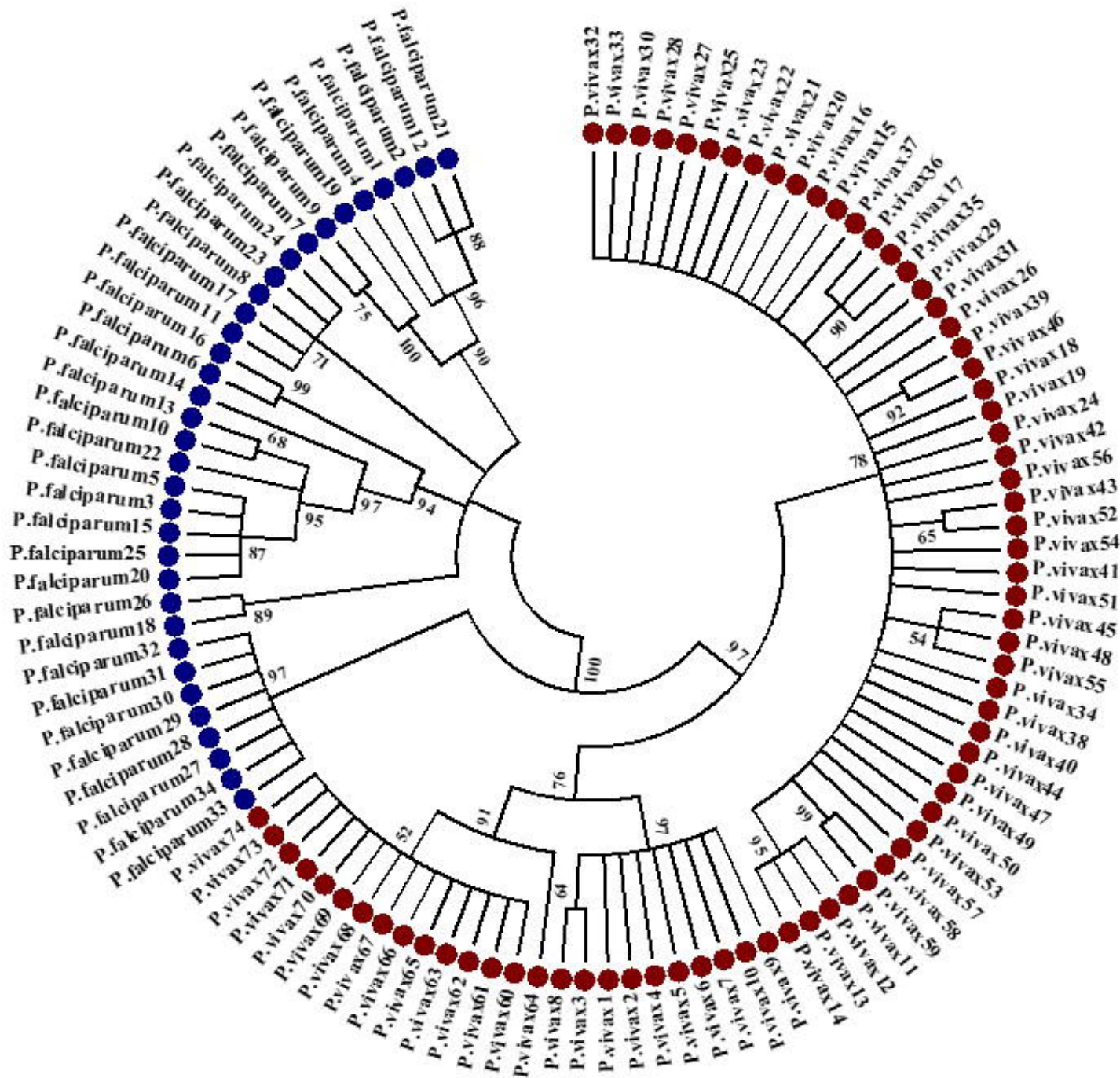
Confirm the filtered sequences overlap the same  
region of the rDNA 18S reference sequence library  
(screen.seqs command)

Classify the sequences into either of the two  
species (*P. falciparum* and *P. vivax*)  
(classify.seqs command)

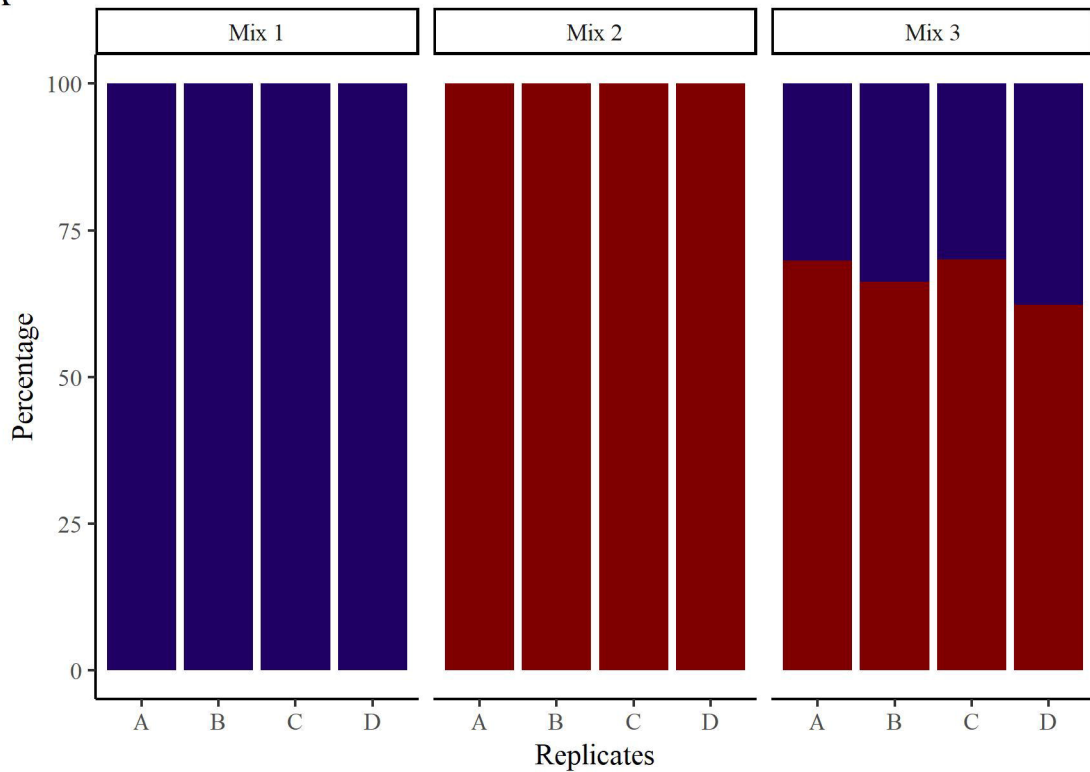
### Step 2

Count list of the consensus sequences for each  
parasite samples based on the total numbers of  
filtered sequences (unique.seqs command)

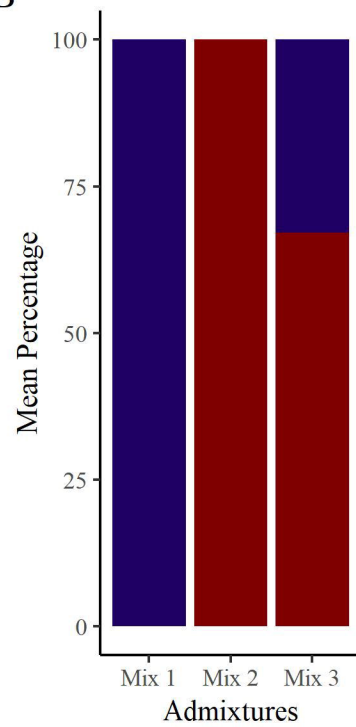
Count list was used to create the FASTQ files of  
the consensus sequences of each sample  
(split.groups command)



A

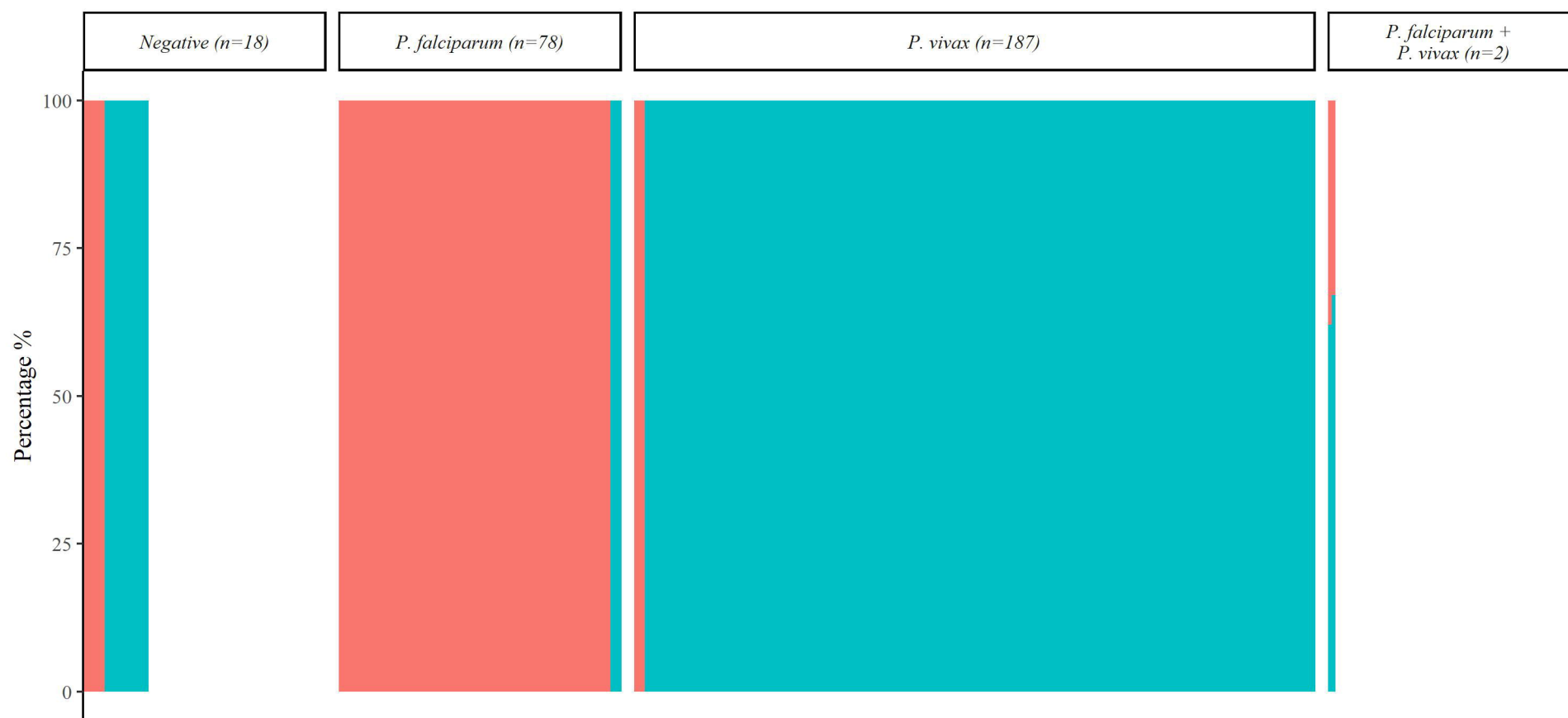


B



■ *P. falciparum* ■ *P. vivax*

**RDT**



**Illumina MiSeq**



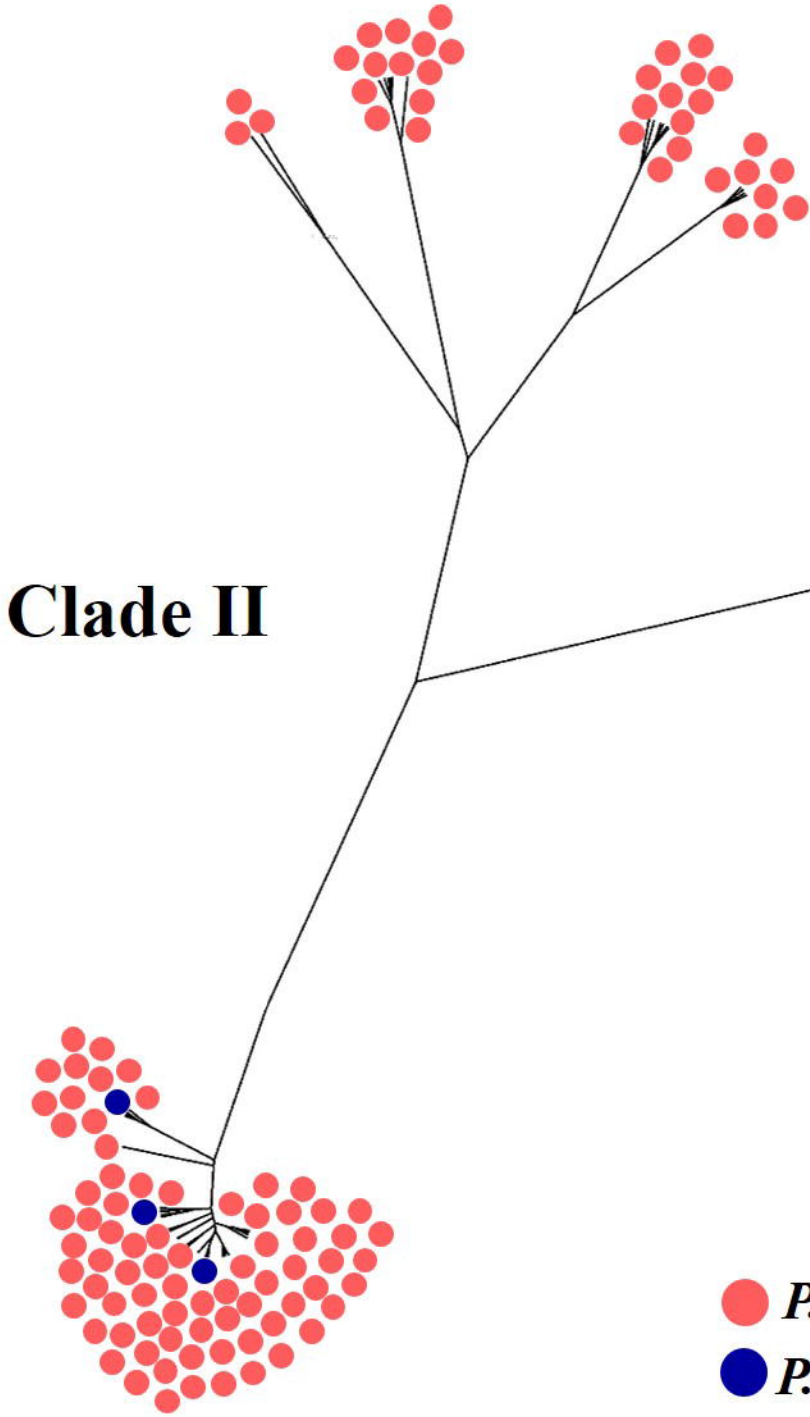
■ *P. falciparum* ■ *P. vivax*

RDT performance, using Illumina MiSeq as a gold standard:

	Predictive Value (95% CI)	Category-Specific Classification Probability (95% CI)
RDT Negative	0.816 (0.724 - 0.883)	1*
RDT <i>P. falciparum</i>	0.962 (0.860 - 0.990)	0.893 (0.807 - 0.943)
RDT <i>P. vivax</i>	0.984(0.938 - 0.996)	0.924 (0.881 - 0.953)
RDT <i>P. falciparum</i> + <i>P. vivax</i>	1*	1*

\* It was not possible to calculate confidence intervals for these values due to the absence of false classifications in this dataset.

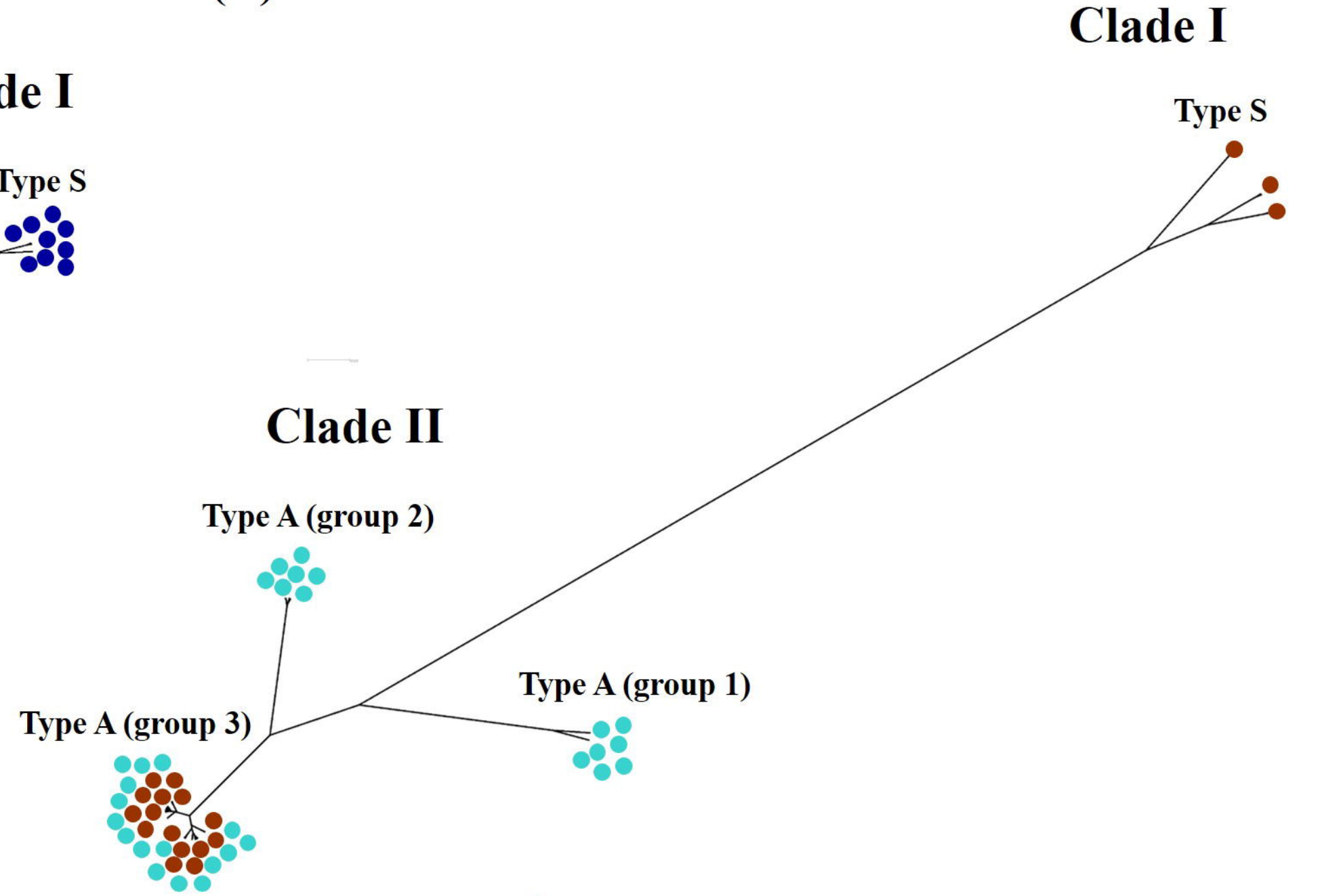
**(A)**  
Type A (group 2)



● *P. falciparum* (field samples)  
● *P. falciparum* (NCBI GenBank)

Type A (group 1)

**(B)**



● *P. vivax* (field samples)  
● *P. vivax* (NCBI GenBank)

Clade I

Type S